Zhou, X., Lai, D. and Chen, Q. 2020. "Thermal sensation model for driver in a passenger car with changing solar radiation," *Building and Environment*, 183: 107219

Thermal Sensation Model for Driver in a Passenger Car with Changing Solar Radiation

Xiaojie Zhou[a], Dayi Lai[b,a*], Qingyan Chen[c]

[a]*Tianjin Key Laboratory of Indoor Air Environmental Quality Control, School of Environmental Science and Engineering, Tianjin University, Tianjin, China*

[b]*Department of Architecture, School of Design, Shanghai Jiao Tong University, Shanghai 200240, China*

[c]*School of Mechanical Engineering, Purdue University, West Lafayette, IN, USA*

HIGHLIGHTS

- Studied human thermal sensation in passenger car under actual outdoor driving conditions.
- Evaluated the applicability of existing thermal sensation models to cars under driving conditions.
- Analyzed the effect of sudden changes in solar radiation on human thermal sensation.
- Developed a new model to predict thermal sensation in a car under driving conditions.

ABSTRACT

Thermal sensation in cars is different from that in buildings. Transient, asymmetric solar radiation and transient, non-uniform air temperature are the main causes of the difference. This investigation conducted human subject tests with 24 subjects, 62 trials under three outdoor driving conditions. These three driving conditions refers to 1) highly transient environments during the cool-down phases in summer, 2) highly transient environments during the warm-up in winter, and 3) sudden changes in solar radiation in shoulder season. Then the data were used to evaluate the performance of four thermal sensation models: the predicted mean vote model, the dynamic thermal sensation model, a model from the University of California, Berkeley, and a transient outdoor thermal sensation model. The results of the evaluation indicated that none of the models could accurately predict thermal sensation in a car. The sudden change in solar radiation experienced by the driver was identified as an important factor in this discrepancy. Therefore, this study proposed a new thermal sensation model that incorporates the change in the driver's thermal load caused by a sudden change in solar radiation as a predictor. This investigation verified the validity of the new model in a transient and non-uniform vehicular thermal environment.

Keywords: Vehicle thermal comfort; Model development; Solar radiation; Non-uniform, Transient

1. Introduction

An increasing number of people in China are using passenger cars for commuting. It is essential to quickly attain an acceptable comfort level inside cars during short commutes so that drivers will be more focused and alert [1]. A comfortable thermal environment can also alleviate fatigue, reduce irritability, and improve driving safety [2]. Over the past ten years, the number of studies on thermal comfort in vehicles has progressively increased. The main focus of these studies has been the creation of an environment that is thermally comfortable for passengers. Many studies have used thermal sensation models, such as the predicted mean vote (PMV) model [3],[4], a model developed by the University of California, Berkeley (UCB) [5],[6],[7], and the dynamic thermal sensation model (DTS) [8],[9],[10].

Although the PMV model was originally developed for buildings, it has frequently been applied in vehicles. Zhang [11] found that PMV can be accurately used to predict thermal comfort levels in parked cars. However, unlike the relatively uniform thermal environment in parked cars, the thermal environment in moving cars is non-uniform because of rapid change in solar radiation and non-uniform air temperature. As a result, some researchers have modified the PMV model for vehicular environments. For instance, Ingersoll et al. [12] used an area-weighted PMV by considering PMV for head, torso, and feet. Matsunaga et al. [13] employed an average equivalent temperature by weighting the surface area of the head (0.1), abdomen (0.7), and feet (0.2) when calculating PMV in a car. The UCB and DTS models, which are more advanced than PMV, consider local and dynamic influences. Several researchers have employed the UCB model ([6], [14], [15]) and the DTS model [16]. Although these models appear to be popular, they have been applied in simulated thermal environments in laboratories, which could differ considerably from actual driving environments.

Since actual driving environments are more complex than one that is simulated in a laboratory, it is not clear whether the models described above can predict actual thermal sensation with high accuracy. In addition, the models do not directly consider the effect of solar radiation, which may play a very important role in thermal comfort in driving environments [17], [18], [19]. For example, Rugh and Farrington [20] claimed that typically 50% to 75% of the thermal energy entering the car cabin was due to transmitted and absorbed solar energy from the glazing. Windshield alone accounted for more than 40% of heat transmitted into the cabin [21]. Therefore, the incident solar radiation transmitted through the glass of the car was the main cause of high cabin temperature, and may cause a change in thermal sensation. Hodder and Parsons [22] found that the thermal sensation vote increased by one unit, when simulated solar radiation (instead of real solar radiation) increased by 200 W/m^2. Ozeki et al. [23] discovered that the use of solar control glass can reduce the thermal sensation vote by one to two units compared to ordinary glass under outdoor parking conditions. However, solar radiation absorbed by drivers and passengers under driving conditions can change dramatically when the vehicle is exposed to sun or shadow or when it changes direction. To date, the effect of solar radiation change on thermal sensation has not been thoroughly studied.

Many studies have used standard EN ISO 14505 [24], [25], [26]. The evaluation indexes used in standard ISO14505 are predicted mean vote (PMV) [24] and equivalent temperature [25]. But the effect of sudden change of solar radiation could not be considered in PMV model or equivalent temperature [27].

To evaluate the applicability of existing thermal sensation models to cars under driving conditions, this study collected data by means of human subject tests. The data was also used to develop and validate a model that considers the influence of solar radiation on thermal sensation.

2. Research Method

2.1 Heat exchange between a human body and its surroundings in a vehicle

The heat exchange between a human body and its surroundings in a car is more complex than that inside a building. Therefore, it was necessary to analyze the heat exchange inside a vehicle. The use of automotive air conditioners and the impact of dynamic weather conditions make the thermal environment inside a car non-uniform and transient [28], [29]. The air temperature and velocity surrounding the human body have large variations, and the body may receive transient, asymmetric solar radiation [30]. Therefore, the heat exchange for each segment of the body should be considered separately. The thermal load of segment i of a human body (*TL (i)*) in a vehicle can be expressed as follows [31]:

$$TL(i) = \left[M(i) - W(i)\right] + RS(i) - \left[RL(i) + C(i) + E_{sk}(i) + C_{res}(i) + E_{res}(i)\right] \quad (1)$$

where M is the metabolic rate (W/m^2) that was set to 1.3 met (or 80 W/m^2) under driving conditions; W the rate of mechanical work (W/m^2), which is 0 W/m^2 under driving conditions; RS the rate of shortwave radiation exchange (W/m^2); RL the rate of longwave radiation exchange (W/m^2); C the rate of convective heat exchange (W/m^2); E_{sk} the rate of evaporative heat loss from the skin (W/m^2); and C_{res} and E_{res} the rates of convective and evaporative heat loss, respectively, from respiration (W/m^2). By area-based weighting, the thermal load for the body as a whole is calculated as:

$$TL = \sum TL(i) \cdot A(i) / ADu \quad (2)$$

where $A\ (i)$ is the area of the ith segment, and ADu the Dubois area of a standard person, which is 1.86 m^2 [32]. During driving, one part of the thermal load changes gradually (TL_g) and the other suddenly (TL_s) because of frequent changes in solar radiation (RS). Therefore, to facilitate analysis, the human body thermal load in the car is further divided into two parts, as follows:

$$TL = TL_g + TL_s \quad (3)$$

$$TL_g = \left[M - W\right] - \left[RL + C + E_{sk} + C_{res} + E_{res}\right] \quad (4)$$

$$TL_s = RS \quad (5)$$

Of the heat transfer terms in Eq. (1), the shortwave and longwave radiation are the most complicated. The rate of short-wave radiative heat gain *RS* is the summation of the direct solar radiative heat gain (RS_{dir}), the first reflection of direct solar radiation heat gain (RS_{ref}), and the diffuse solar radiative heat gain (RS_{dif}):

$$RS(i) = RS_{dir}(i) + RS_{ref}(i) + RS_{dif}(i) \tag{6}$$

The direct shortwave radiation, $RS_{dir}(i)$, is calculated as:

$$RS_{dir}(i) = \alpha(i) \cdot f_{p,dir}(i) \cdot G_{dir} \tag{7}$$

where α is the short-wave absorptivity at the human body surface, G_{dir} the direct solar radiation intensity that falls on the glass surface (W/m^2), and $f_{p,dir}$ the projection area factor for direct shortwave radiation, which is expressed as [33]:

$$f_{p,dir}(i) = \sum_k \tau_k \cdot FD_k(i) \tag{8}$$

where τ_k is the transmissivity of car glass k, and $FD_k(i)$ the directional view factor representing the fraction of the direct solar flux entering through window k and received by segment i.

The first reflection of direct shortwave radiation, $RS_{ref}(i)$, is calculated as:

$$RS_{ref}(i) = \alpha(i) \cdot f_{p,ref}(i) \cdot G_{dir} \tag{9}$$

where $f_{p,ref}$ is the projection area factor for first reflection of direct shortwave radiation. This factor is expressed as [33]:

$$f_{p,ref}(i) = \sum_k \tau_k \sum_j \rho_j \cdot FR_{k,j}(i) \tag{10}$$

where ρ_j is the reflection coefficient for shortwave radiation of surface j, and the distribution factor $FR_{k,j}(i)$ represents the fraction of the direct flux emitted by window k and reflected by j onto i when the surface j is assumed perfectly reflecting.

The diffuse part of the shortwave radiation, $RS_{dif}(i)$ (W/m^2), is calculated as [33]:

$$RS_{dif}(i) = \alpha(i) \cdot f_{p,dif}(i) \cdot G_{dif} \tag{11}$$

where G_{dif} is the diffuse solar radiation intensity that falls on the glass surface (W/m^2), and $f_{p,dif}$ the projected area factor for diffuse solar radiation. This factor is expressed as [33]:

$$f_{p,dif}(i) = \sum_k \tau_k \cdot F_k(i) \tag{12}$$

where F_{ki} is the percentage of the diffuse solar flux going from window k to a segment i, which is determined according to the classic hypothesis of isotropic diffuse radiation [33]. The $f_{p,dir}$, $f_{p,ref}$ and $f_{p,dif}$ depend on body posture and angles between the human body and the sun. For a given posture, the projected area factor is a function of azimuth (θ) and altitude (β) angles and the shading effects caused by the vehicle envelope, which are calculated by the TAItherm program [34].

The radiant model should be used to describe local longwave radiant heat transfer (*RL(i)*) on different segments of the body in a highly transient, non-uniform thermal condition such as a vehicle. These *RL(i)* can then be incorporated into a thermal comfort model to predict thermal sensation [35]. The longwave radiant heat transfer between human body segments and surrounding surfaces is calculated according to the Stefan-Boltzmann law as follows [31]:

$$RL(i) = \varepsilon_{sf}(i) \cdot \sigma \cdot \sum_{j=1}^{m} \varepsilon_{sr}(j) \cdot f_{cl}(i) \cdot \psi_{sf(i)-sr(j)} \left[T_{sf}(i)^4 - T_{sr}(j)^4 \right] \tag{13}$$

where $\varepsilon_{sf}(i)$ is the emissivity of body segment i, σ the Stefan-Boltzmann constant (5.67×10^{-8} ($W/m^2/K^4$)), $\varepsilon_{sr}(j)$ the emissivity of the vehicle surface j around the body, $f_{cl}(i)$ the clothing area factor of segment i, and $\psi_{sf(i)-sr(j)}$ the angle factor between body segment i and surrounding surface j, which is calculated by a finite element method by Tanabe [36], [37] and Thellier [38]. The $T_{sf}(i)$ is the surface temperature of body segment i, (*K*), which is either the clothing surface temperature if the segment is clothed, or the skin temperature if the segment is unclothed. The $T_{sr}(j)$ is the temperature of the surface around the human body (vehicle interior surface) j, (*K*).

The convective heat exchange, *C*; the evaporative heat loss at the skin, E_{sk}; and the convective and evaporative heat transfer from respiration, C_{res} and E_{res}, respectively, are calculated as specified by the American Society of Heating, Refrigerating, and Air-Conditioning Engineers (ASHRAE) [31].

2.2 Human subject tests

To collect data for assessing the existing models and developing a new model for vehicles under actual driving conditions, we conducted human subject tests in a Nissan Tiida passenger car (2014 model). The color of the car exterior was red and the interior decor and upholstery was light grey. The size of this model was rather typical in China. The tests were performed in summer, winter, and the shoulder season, from July 17, 2017, to May 22, 2019, in Tianjin, China. All experiment was performed at the same time of each day from 10:00 a.m. to 3:00 p.m. This study recruited 24 healthy subjects to evaluate thermal comfort in a car. Three types of trials were performed: 1) highly transient environments during the cool-down phases in summer, 2) highly transient environments during the warm-up in winter, and 3) sudden changes in solar radiation in shoulder season. Each subject participated in at least two tests. A total of 24 tests were conducted in summer. In 16 of the 24 tests, only one subject sat in the driver's seat, and in the rest tests, two subjects sat in the driver's seat and in the front passenger seat, respectively. A total of 15 tests were conducted in winter and shoulder season when only one subject sat in the driver's seat. Table 1 presents physiological and clothing information about the participants in different seasons. The number of subjects in each season exceeded eight, as required by EN ISO 14505 1-3 [24], [25], [26] for evaluating thermal comfort in a vehicle.

Table 1. Subject information in each season

Season	Number of subjects	Number of trails	Height (cm)	Weight (kg)	Age	Clothing(clo)
Summer	16 (8 male, 8 female)	32	171±4.6	65±4.7	34±10	0.5
Winter	15 (9 male, 6 female)	15	172±3.8	65±5.2	34±9	1.5
Shoulder season	15 (7 male, 8 female)	15	169±5.6	65±3.3	39±5.6	0.67

The subjects were local residents acclimated to the local climate, and had more than five years of driving experience. To increase the accuracy of the test results, it was ensured that the subjects had enough sleep at night before the test. In addition, they were not allowed to take any food or drug that may affect the cognitive function.

Figure 1 depicts the procedure for the subject tests. Before the subjects entered the vehicle, they rested in a preparation room with ambient temperature close to the neutral level (26°C for summer and shoulder season, and 20°C for winter) and remained in the room for 30 minutes to achieve a neutral thermal state. During their stay in the room, all the subjects gave consent prior to their participation in the experiment and were briefed on both the withdrawal criteria and the experimental procedure.

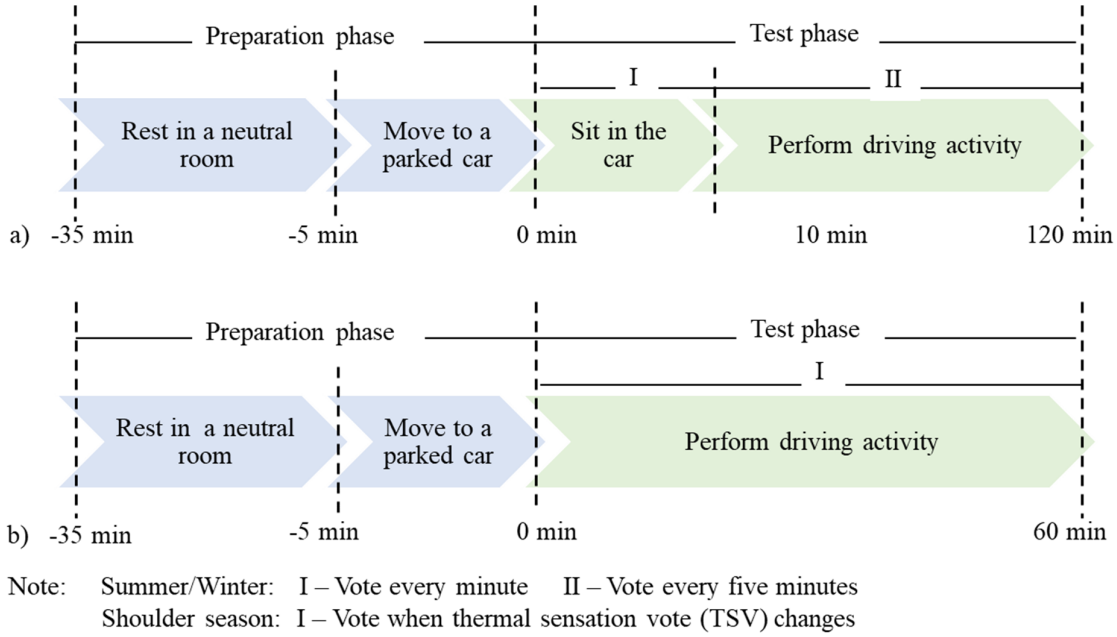

Fig. 1. Experimental protocol: a) summer/winter, b) shoulder season.

When one or two subject(s) entered the car, they seated in the front seat(s) of the car. The air-conditioning system was turned on immediately to cool/heat the interior space using the recirculation mode. The air supply mode was set to “panel vent” in summer and shoulder season and “panel vent + foot vent” in winter. The fan speed was set at the medium level with

an airflow rate of 0.072 m^3/s together with the target cabin air temperature. During the test phase in the vehicle, the subjects provided their thermal sensation vote (TSV) according to the ASHRAE seven-point scale (−3 = cold, −2 = cool, −1 = slightly cool, 0 = neutral, 1 = slightly warm, 2 = warm, and 3 = hot). As McIntyre [39] found that, in general people cannot deal with more than about seven levels of sensation without confusion. The voting frequency and driving route for the shoulder season was different from that for summer/winter. In summer and winter, the tests focused on the human thermal response under a gradually changing thermal environment. The initial thermal environment in the vehicle deviated greatly from neutral, and operation of the air conditioner caused a change in air temperature. The subjects voted their thermal sensation every minute during the first ten minutes. Because of the frequent voting, for safety reasons, the subjects sat in the car and did not perform any driving activity. After the first ten minutes, the subjects started to drive on a north-south road with a length of about 10 km, go back and forth, and then provided their TSV every five minutes. Since a long time was needed for the cabin thermal environment to reach a steady state in summer and winter, the subjects spent two hours in the vehicle. For the experiment during the shoulder season, the air temperature in the vehicle was close to neutral, and the use of the air conditioner did not cause a large change in the interior air temperature. The tested vehicle was driven on a road with alternating sun and shade, and the main objective of the test in the shoulder season was to investigate the subjective thermal response to sudden changes in solar radiation. Therefore, the subjects were asked to provide their votes whenever they felt changes in thermal sensation. A total of 1721 valid votes were collected, with 908, 495, and 318 votes in summer, winter, and the shoulder season, respectively.

Table 2. Interior air temperatures around the subjects (#1–#9) and interior surface temperatures (#10–#19)

1#	2#	3#	4#	5#	6#	7#	8#	9#
Driver's face	Driver's lower arm	Driver's lower leg/feet	Passenger 's lower leg/feet	Driver's head	Passenger 's head	Driver's upper arm	Driver's upper leg	Passenger 's upper arm

10#	11#	12#	13#	14#	15#	16#	17#	18#	19#
Wind shield	Dash board	Driver side window	Cei-ling	Driver seat cushion	Driver seat back	Passenger seat cushion	Passenger seat back	Passenger side window	Floor

During the subject tests, several parameters of the thermal environment—air temperature, surface temperature, and relative humidity (*RH*) at the position of the subject's head—inside the vehicle cabin were continuously recorded. The monitoring of air temperature and interior surface temperature was achieved with the use of 19 thermocouples, as shown in Figure 2(a); the measurement locations are listed in Table 2. In addition, air velocity (V_a) of different segments of the human body were measured under parking condition. Sensors were installed

on the top of the car to collect outside air temperature, relative humidity, and horizontal solar irradiance data for the outside thermal environment as shown in Table 3.

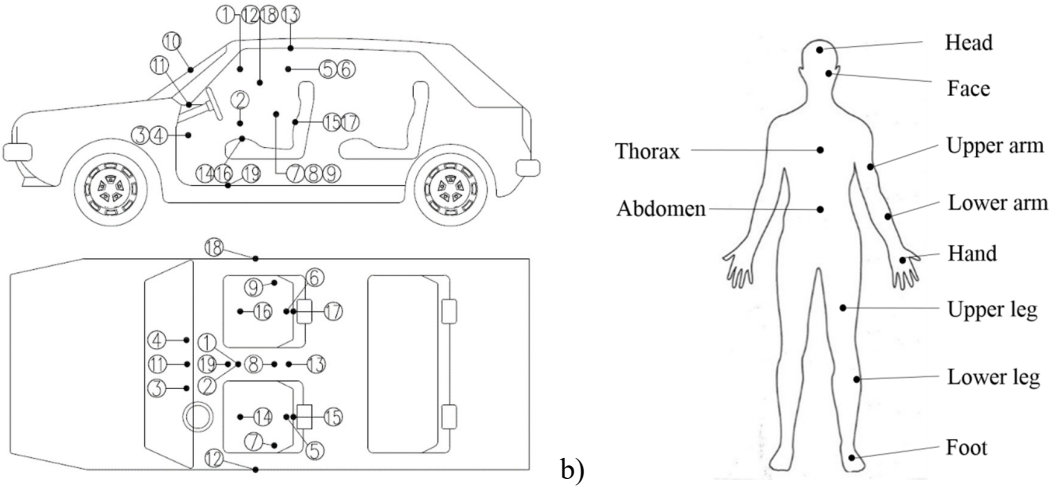

a) b)

Fig. 2. Positions of thermocouple measurements in the experiment: a) interior air temperatures around the subjects (#1–#9) and interior surface temperatures (#10–#19), and b) skin temperatures of subjects.

To study the impact of cabin thermal environment on a human body, we used 10 thermocouples to measure the skin temperature on different parts of the subjects' bodies, as shown in Figure 2(b). The mean skin temperature was calculated by weighting the skin temperature on the ten measured body parts according to the surface areas of the parts. The thermocouples were connected to a portable data logger. Table 3 provides the specifications of the instruments used in the subject tests.

Table 3. Technical specifications of the sensors used to measure inside and outside environmental parameters and skin temperatures.

Parameter*	Sensor type	Range	Accuracy	Measurement frequency
G, outside	S-LIB-M003	0 to 1280 W/m^2	±10 W/m^2 or ±5%	10 sec.
T_a, outside	S-THB-M002	-40 to 75°C	±0.2 K at 20°C	10 sec.
RH, outside	S-THB-M002	0 to 100%	±3%	10 sec.
T_{sk}	TT-K-30-SLE	0 to 350°C	±1.1°C or ±0.4%	1 sec.
T_a, inside	TT-K-30-SLE	0 to 350°C	±1.1°C or ±0.4%	1 sec.
RH, inside	HOBO U12	5 to 95%	±2.5% from 10 to 90%	10 sec.
V_a, inside	AirDistSys 5000	0.05 to 5 m/s	±0.02 m/s ±1%	1 sec.
T_{sur}, inside	TT-K-30-SLE	0 to 350°C	±1.1°C or ±0.4%	1 sec.

* G = total radiation, T_a = air temperature, RH = relative humidity, T_{sk} = skin temperature, V_a = air velocity, T_{sur} = surface temperature.

2.3 Evaluated thermal sensation models

The data collected from the subject tests was used to assess the performance of current thermal sensation models under actual driving conditions. In our literature survey, we identified three models that could be used to evaluate thermal comfort in vehicles: the predicted mean vote (PMV) model by Fanger [3], the dynamic thermal sensation (DTS) model by Fiala [8], [9], and the University of California, Berkeley (UCB) comfort model by Zhang [5], [6], [7]. Since these models had been not developed using data obtained in a vehicular environment, it was essential to assess their performance in cars. Because vehicles are directly exposed to the outdoor climate, we also selected an outdoor thermal comfort model (Lai's model) [40], [41], [42] for evaluation.

The PMV model was based on the human energy budget under steady-state thermal conditions. It predicts the mean thermal sensation vote of a group of people using environmental and personal parameters as input. The DTS model was developed by Fiala [8], [9], by regressing a large amount of pre-existing human subject test data. It is a transient thermal sensation model used for spatially uniform conditions. The UCB model was originally intended for studying the thermal comfort in a non-uniform environment. It was based on the regression of a large amount of data from experiments in which local cooling/heating was applied to different segments of subjects' bodies. The UCB model first predicts the thermal sensation for a local segment, and then the whole-body thermal sensation is obtained by integrating the local sensations. Meanwhile, Lai's model was based on the regression of a large amount of experimental data obtained in different outdoor thermal environments. Table 4 lists the air temperature range under which the data was obtained for each model, and the model's input parameters.

Table 4. General information about the thermal sensation models.

Model	Air temperature range (ºC)	Input parameters*	References
PMV	19–28	*TL, Met*	Fanger [3], Chap. 4, Eqs. (25), (40) and (41)
DTS	10–48	$\Delta T_{sk,m}$, ΔT_{cr}, $dT_{sk,m}/dt$	Fiala et al. [9], Eqs. (1)–(10)
UCB	20–32	$\Delta T_{sk,m}$, $\Delta T_{sk,i}$, $dT_{sk,i}/dt$, dT_{cr}/dt	Zhang et al. [5], Eq. (5)
			Zhang et al. [7], Section 1.3.1
Lai's	0–35	$\Delta T_{sk,m}$, *TL*, $dT_{sk,m}/dt$	Lai et al. [42], Eqs. (3) and (4)

*TL - thermal load, Met - Metabolic rate, $T_{sk,m}$ - mean skin temperature, T_{cr} - core temperature, $T_{sk,i}$ - skin temperature for the i^{th} segment, dT_{cr}/dt, $dT_{sk,i}/dt$ and $dT_{sk,m}/dt$ - rates of change of core temperature, mean skin temperature and skin temperature for the i^{th} segment, respectively. Parameters marked by a delta (Δ) are error signals, i.e., the difference between the value of the parameter under the actual conditions and the value under thermo-neutral conditions.

Mean skin temperature ($T_{sk,m}$) is an area-weighted value, i.e.

$$T_{\mathrm{sk,m}} = \int T_{sk} dA_{sk} / ADu \tag{14}$$

where T_{sk} is the local skin temperature and dA_{sk} the corresponding local surface area on a body element of the human.

The performance of the models was assessed by means of three parameters: Pearson's correlation coefficient (R), the percentage of correct prediction, and the root-mean-square error (RMSE). The percentage of correct prediction in this study is defined as the percentage of predictions with error of less than or equal to one unit of the voting scale. The root-mean-square error (RMSE) was calculated according to the following equation:

$$RMSE = \sqrt{\frac{\sum\left(x_{actual} - x_{prediction}\right)^2}{n}} \tag{15}$$

where x_{actual} is the experimental measured value, $x_{prediction}$ is the predicted value, and n is the number of observations.

3. Results

This section first provides descriptive results for the thermal environment and skin temperature in the car under driving conditions. Next, the performance evaluation results for the four selected thermal sensation models are presented. Finally, we discuss the development and validation of the thermal sensation model in the car under driving conditions.

3.1 Descriptive results from the subject tests

To demonstrate the overall trends in thermal environment and thermal comfort in a vehicle, this sub-section discusses the air and surface temperatures, relative humidity in the car and the mean skin temperature and thermal perception of the subjects in all tested cases in each season.

As shown in Figure 3(a), the initial air temperature in the car cabin in summer greatly deviated from the neutral level, with a median value of 39.8 ºC. After the car's air conditioner was turned on, the air temperature changed rapidly to the neutral level. The surface temperature also exhibited a dramatic change in summer, as shown in Figure 3(b). However, because of the thermal inertia of the car, the surface temperature varied less than the air temperature. The average surface temperature changed from 41.5 ºC to 32.3 ºC. The relative humidity varied from 34.1 to 32.8% as shown in Figure 3(c). A fluctuation of relative humidity was found during the first 10 minutes, mainly caused by the startup of the air conditioning system. Then the relative humidity was stable at about 30%. The thermal environment around the subjects in the car greatly influenced their mean skin temperature, which changed from 35.1 ºC to 33.3 ºC in summer, as shown in Figure 3(d). According to Figure 3(e), the median TSV decreased from 2 (warm) at the beginning of exposure to 0 (neutral) quickly during the first 15 minutes, and kept the neutral state to the end.

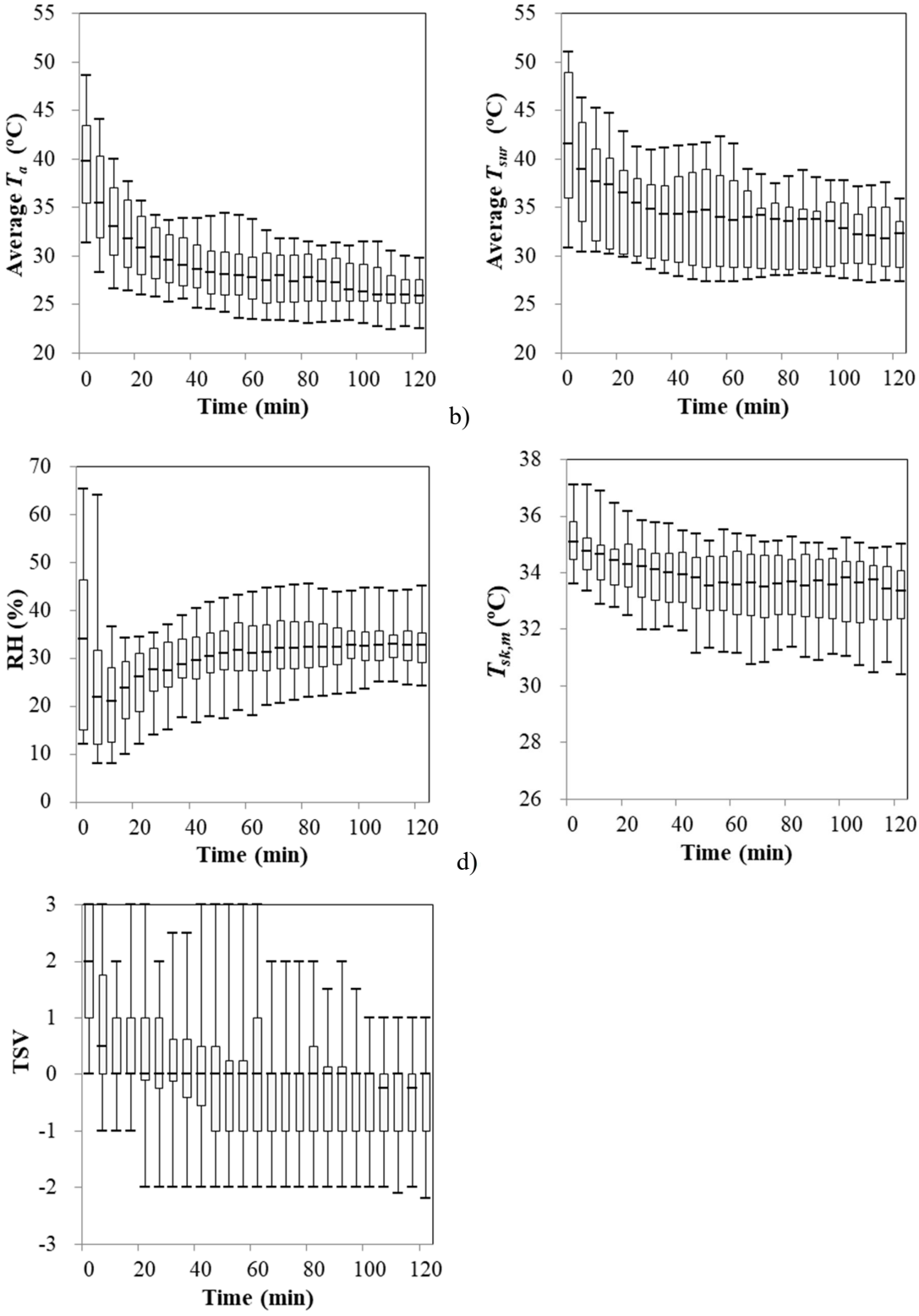

Fig. 3. Box charts of summer experimental results: (a) average air temperature around the subjects; (b) surface temperature around the subjects; (c) relative humidity; (d) mean skin temperature of the subjects; (e) TSV. The horizontal line represents the median value, the upper and lower bounds of the

boxes represent the 25th and 75th percentiles, respectively, and the lower and upper bounds indicate the minimum and maximum, respectively.

Figure 4 displays the experimental results under heating conditions in winter, which were exactly the opposite of the results in summer. The average air temperature varied from 6.9 ºC to 28.6 ºC (Figure 4(a)), while the average surface temperature changed from 3.3 ºC to 21.3 ºC (Figure 4(b)). The relative humidity varied from 27.2 to 21.1% for winter as shown in Figure 4(c). As shown in Figure 4(d), the mean skin temperature changed from 30.2ºC to 34.6 ºC. The change in mean skin temperature in winter (4.2 ºC) was much larger than that in summer (1.8 ºC). There were two main reasons for this difference. First, the air temperature and surrounding surface temperature changed over a smaller range in summer than in winter. Second, under warm conditions, the evaporative heat transfer caused by sweating prevents the skin temperature from becoming too high [43], while under cold conditions, the skin temperature can vary greatly [44]. As shown in Figure 4(e), the median TSV rose from -1 (slightly cool) to 1.5 (between slightly warm and warm). The warm thermal sensation at the end of exposure was due to the high air temperature (28.3 ºC), lower relative humidity (21%) and the thick clothing (1.5 clo) worn by the subjects.

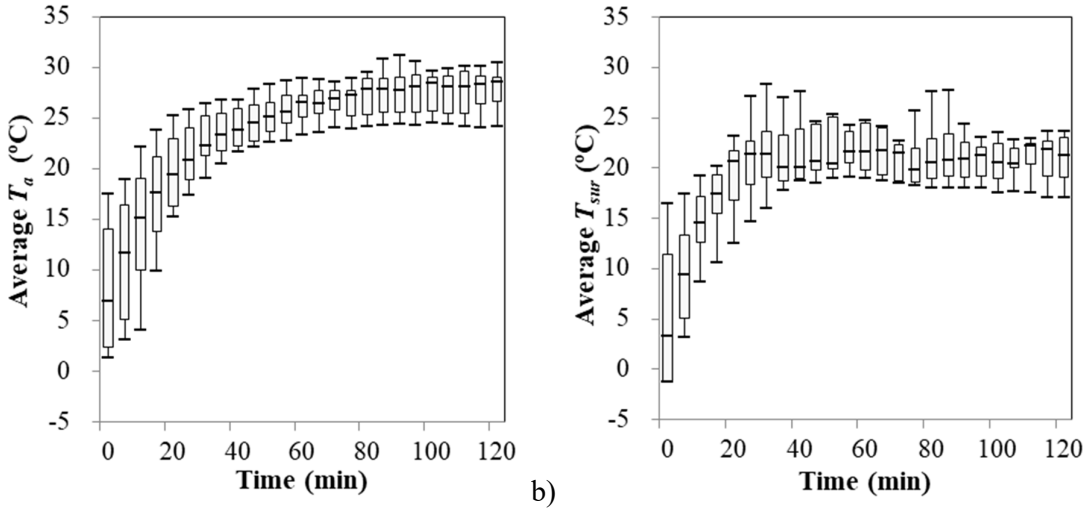

a) b)

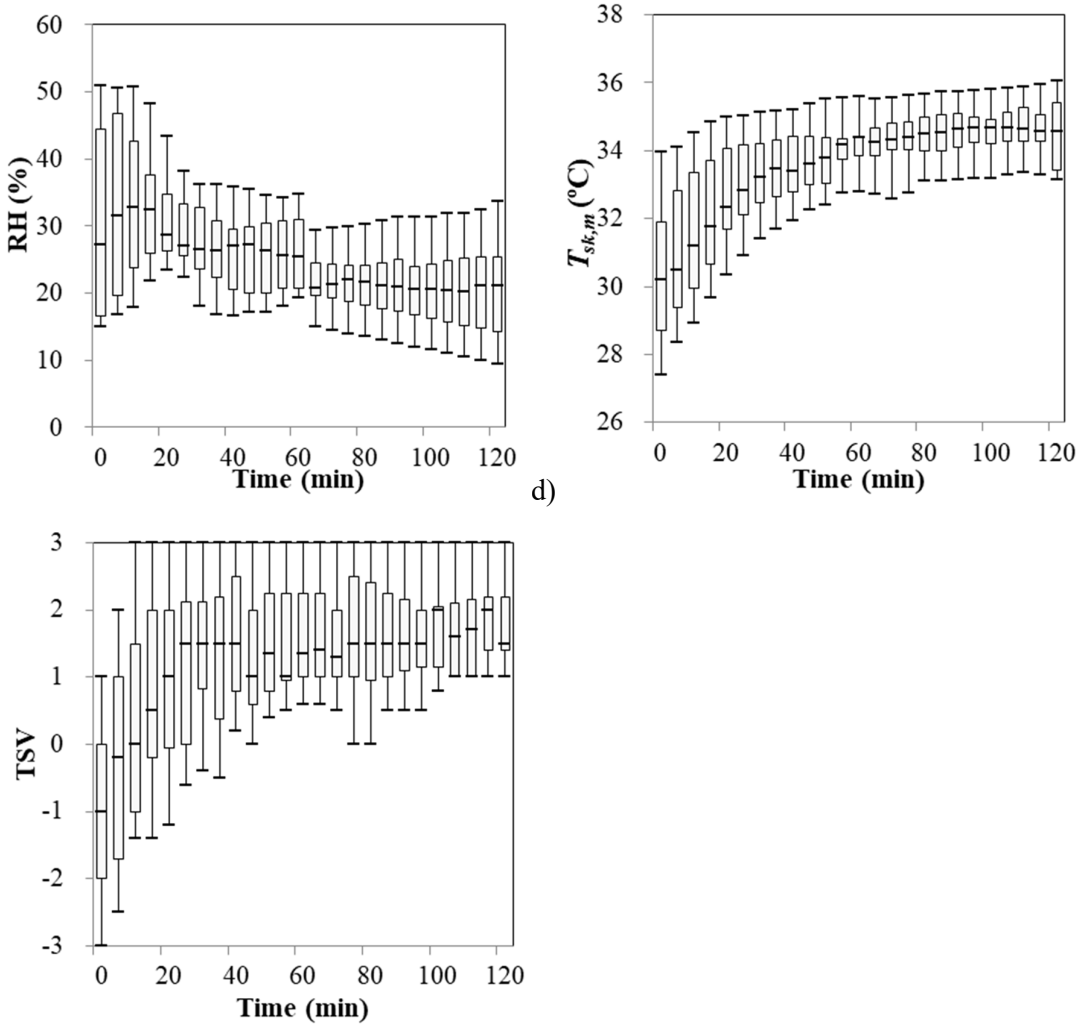

Fig. 4. Box charts of winter experimental results: (a) average air temperature around the subjects; (b) surface temperature around the subjects; (c) relative humidity; (d) mean skin temperature of the subjects; (e) TSV. The horizontal line represents the median value, the upper and lower bounds of the boxes represent the 25th and 75th percentiles, respectively, and the lower and upper bounds indicate the minimum and maximum, respectively.

The above analysis demonstrates that the thermal environment was highly transient during the warm-up and cool-down phases in winter and summer. While in the shoulder season, the median air temperature in the car at the beginning of the test was 26.0 ºC, and its change was within 1 K (Figure 5(a)). The change in average surface temperature was less than 0.5 K (Figure 5(b)), and The relative humidity was stable at 30% during the shoulder season as shown in Figure 5(c). The mean skin temperature remained almost unchanged (Figure 5(d)), during the entire one-hour exposure. Moreover, it can be seen in Figure 5(e) that during the shoulder season, TSV was mainly concentrated between 0 (neutral) and 2 (warm), primarily because the subjects continually experienced sudden changes in solar radiation. The effects of solar radiation on thermal sensation are described in detail below.

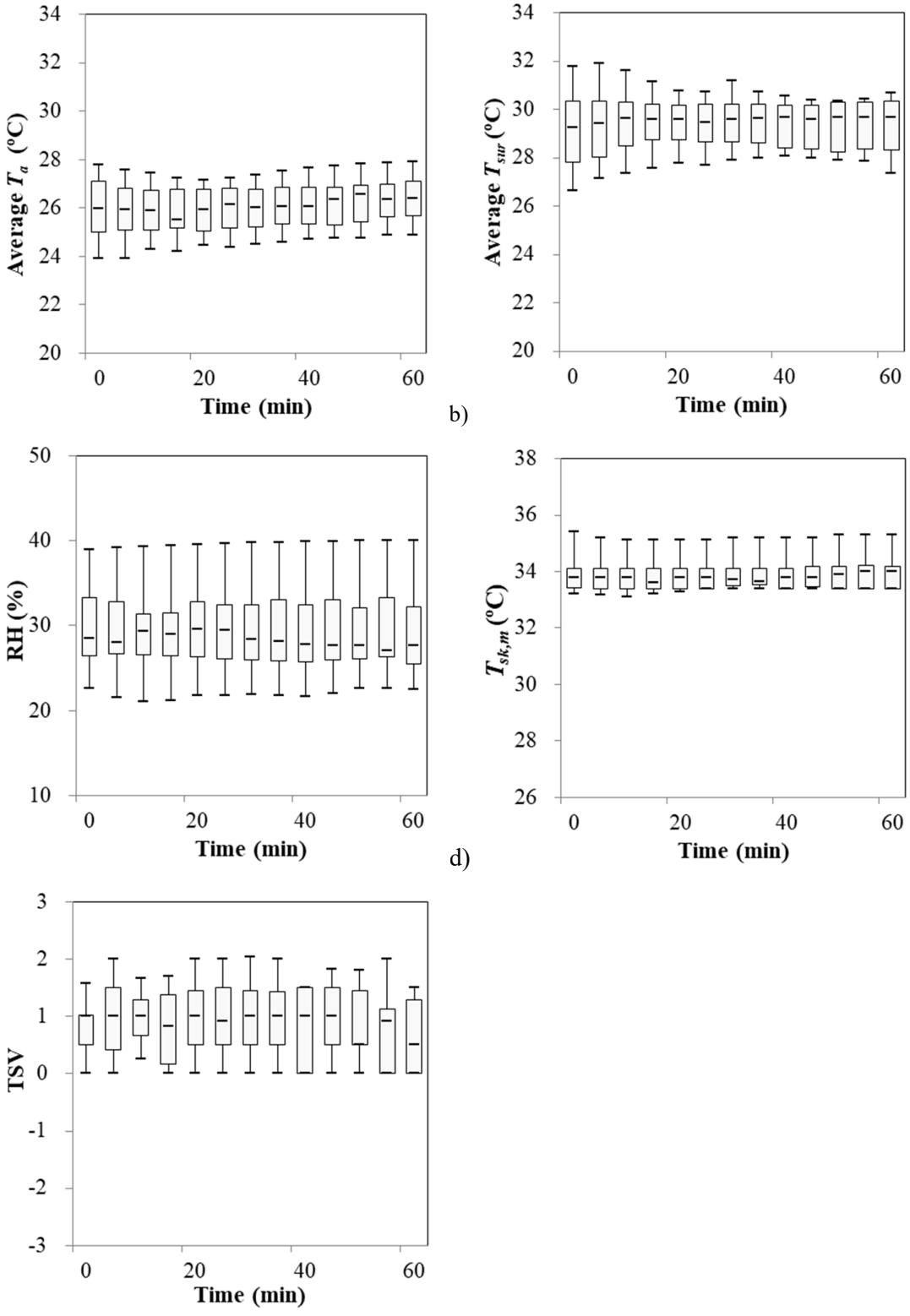

Fig. 5. Box charts of shoulder-season experimental results (a) average air temperature around the subjects, (b) surface temperature around the subjects, (c) relative humidity; (d) mean skin temperature of the subjects; (e) TSV. The horizontal line represents the median value, the upper and lower bounds

of the boxes represent the 25th and 75th percentiles, respectively, and the lower and upper bounds indicate the minimum and maximum, respectively.

Next, Figure 6 shows the impact of solar radiation variations on thermal sensation by presenting the distributions of air and surface temperatures around a typical driver in a test of shoulder season, and his/her skin temperatures, thermal loads, and thermal sensation vote. The temporal variation in air temperature shown in Figure 6(a) was generally within ±1 K, but the vertical air temperature difference between head and lower leg could exceed 3 K. As shown in Figure 6(b), the surface temperature of most parts of the car fluctuated within ±1 K. Two exceptions were the windshield and dashboard, which experienced a fluctuation within 3ºC in surface temperature, primarily because of solar radiation changes when the car was driven alternately along sunny and shaded streets. Figure 6(c) illustrates the changes in skin temperature on the head, face, upper and lower arms, and hands, and the mean skin temperature. Generally, the variations in skin temperatures were small, while the exposed parts (head, face, hand) exhibited higher variation than parts covered by clothing (upper and lower arms, upper and lower legs).

Meanwhile, Figure 6(d) shows the gradual and sudden thermal loads, TL_g and TL_s, calculated by Eqs. (4) and (5), respectively. The TL_g was consistently around 15 W/m^2, while TL_s showed large variations, between 10 and 50 W/m^2, as the vehicle was driven along shaded and sunny segments of the road. Figure 6(d) depicts the thermal sensation vote (TSV). While the thermal sensation was between 0.5 and 2, it can be seen that the TSV fluctuation did not follow the trend of air temperature, surface temperature, or skin temperature. It jumped with the sudden changes of solar radiation. Fluctuating solar radiation in a car was frequently encountered in daily driving, and it had a large impact on thermal comfort. Thus, at a higher thermal load, a warmer sensation was perceived.

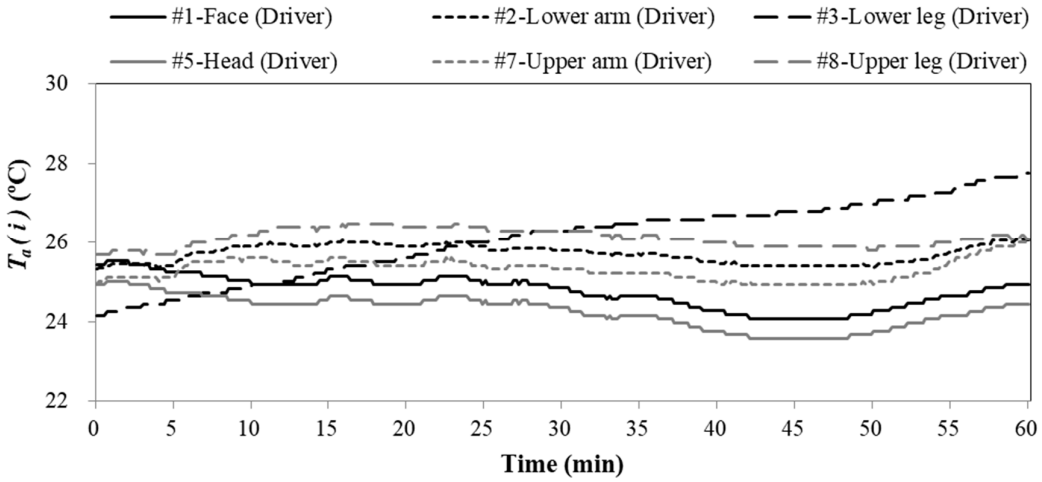

a)

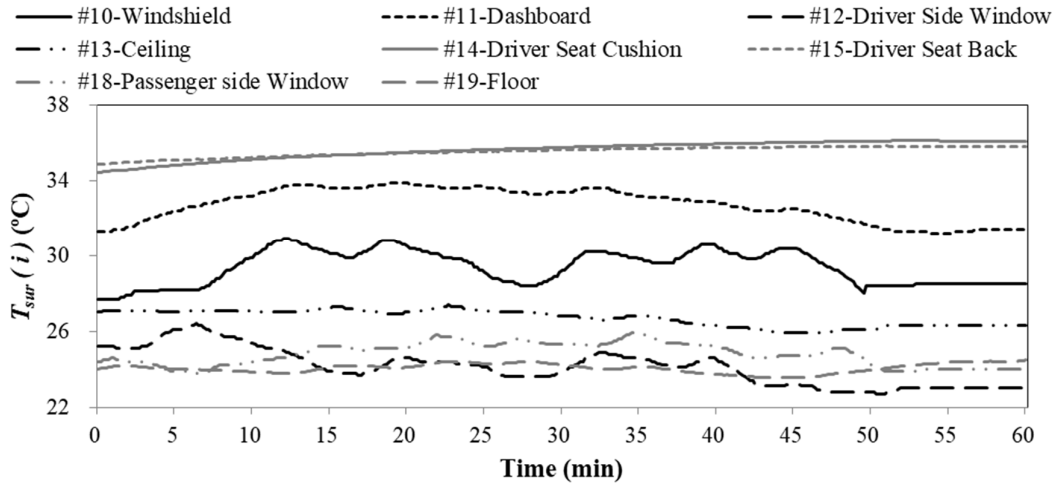

402 b)

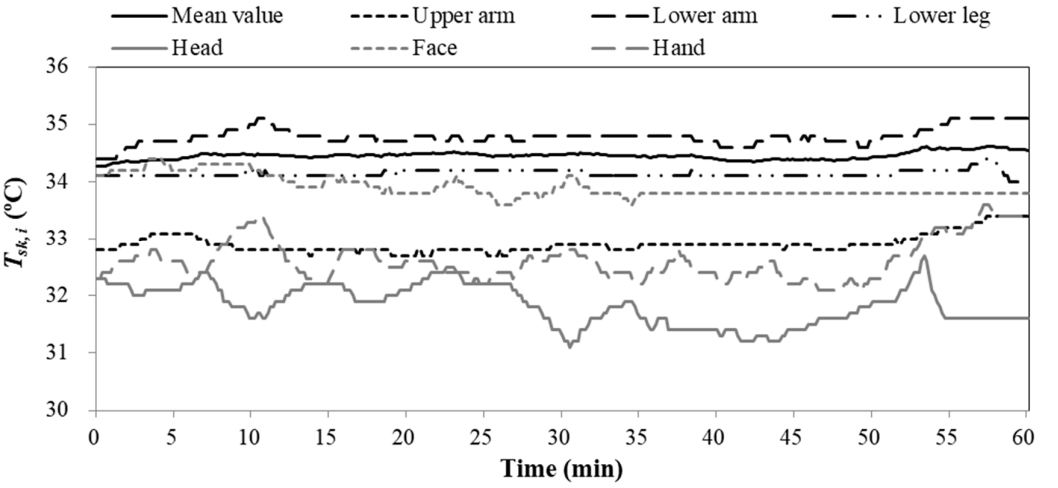

403 c)

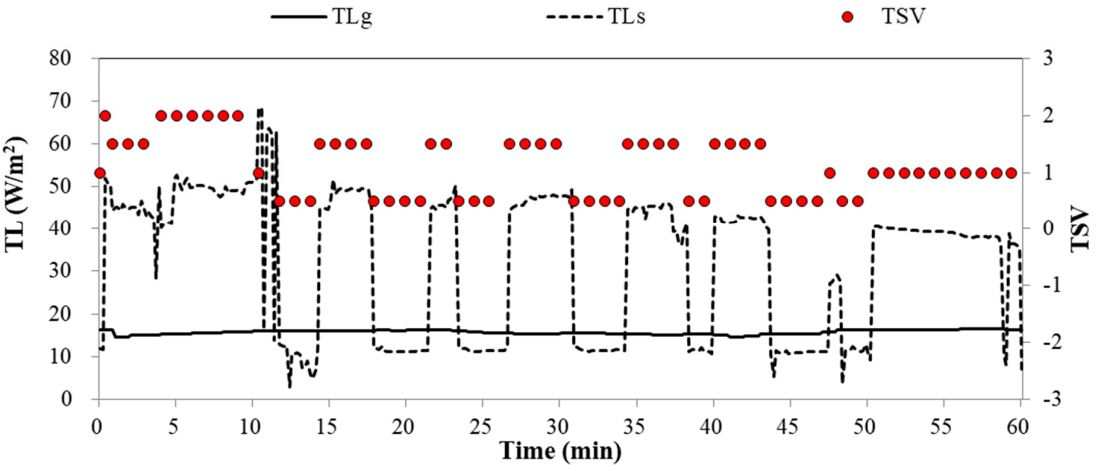

404 d)

405 **Fig. 6.** A tested case in the shoulder season: (a) air temperature, T_a (i), (b) surrounding surface
406 temperature, T_{sur} (i), (c) skin temperature, $T_{sk,i}$, (d) thermal load, TL, and thermal sensation vote, TSV.

407

3.2 Evaluation of thermal sensation models

After this investigation collected the data from the human subject tests, it was used to evaluate the PMV, DTS and UCB models and Lai's model. Figure 7 compares the TSV predicted by the four models with the surveyed TSV for different seasons.

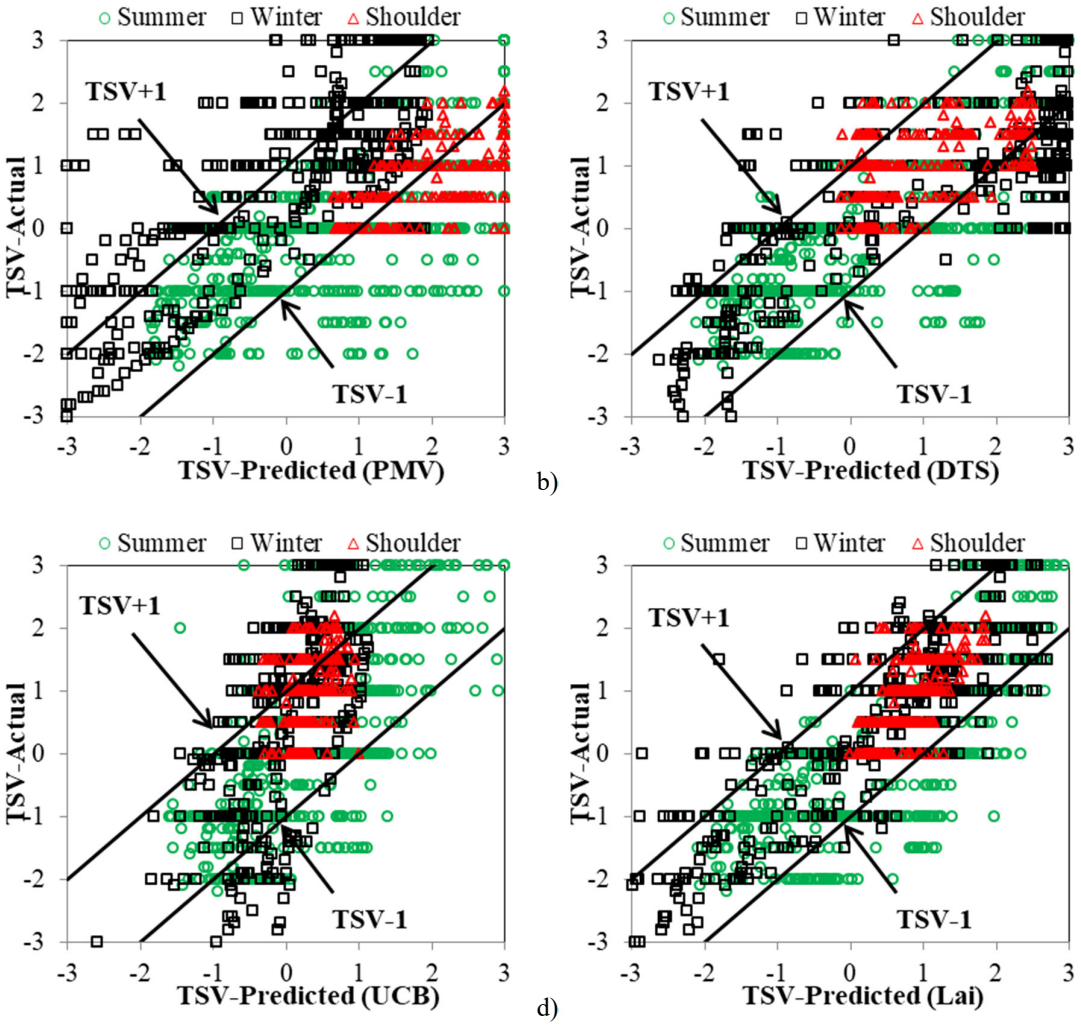

Fig. 7. Comparison of the predicted TSV by (a) PMV, (b) DTS, (c) UCB, and (d) Lai's model with the with the actual TSV obtained from the tests, where "TSV+1" and "TSV−1" are the lines at which predictions are one unit higher or lower, respectively, than the actual value.

Given the difference in the number of participants in three different seasons, statistical analyses were not only conducted for the entire data set, but also respectively for summer, winter and the shoulder season. Table 5 presents the RMSE and the percentage of prediction within an error of one unit for the four models. The RMSE caused by PMV model were 1.65 for summer, 1.27 for winter and 1.49 for shoulder season, respectively. The difference between the predicted value by PMV model and the actual thermal sensation was the largest among the four models. The RMSE of the remaining three models was less than 1 unit in the shoulder season, except the PMV model. This is mainly because, the interior of the car was a

near-neutral environment, and thermal sensation votes were mainly concentrated between 0-2.

The prediction within an error of one unit for PMV model were 64.80% for summer, 57.40% for winter and 38.40% for shoulder season, respectively. The PMV model had the lowest accuracy among the four models, mainly because it was developed for steady-state conditions at the neutral level. Fanger stated that the PMV model should be used with care for indexes below −2 and above +2 and that significant errors can appear in hot environments.

Table 5. Model validation results.

Evaluation index	Season	PMV	DTS	UCB	Lai
RSME	Summer (n=908)	1.65	1.25	1.19	1.20
	Winter (n=495)	1.27	1.26	1.34	0.82
	Shoulder season (n=318)	1.49	0.99	0.82	0.45
Correct percentage (%)	Summer (n=908)	64.80	76.40	77.20	76.30
	Winter (n=495)	57.40	55.40	47.70	77.40
	Shoulder season (n=318)	38.40	68.20	78.30	95.00

Table 6 shows Pearson's coefficient of correlation between thermal sensation vote and four thermal evaluation models. The correlation between the predicted and actual values was the worst for shoulder season. As mentioned earlier, during the transition season, sudden solar radiation was a good explanatory variable for TSV for shoulder season.

Table 6. Pearson′s coefficient of correlation between thermal sensation vote and four thermal evaluation models

	PMV	DTS	UCB	Lai
Summer (n=908)	0.677**	0.742**	0.658**	0.759**
Winter (n=495)	0.744**	0.783**	0.66**	0.836**
Shoulder season (n=318)	0.614**	0.245**	0.376**	0.644**

**$p<0.01$.

This investigation also studied the data from shoulder case in time series. Figure 8 shows the TSV obtained for a shoulder-season case as discussed in Section 3.1. The DTS and UCB models failed to predict the temporal TSV change due to sudden changes in solar radiation because the two models use skin and core temperatures as input, and these parameters changed little with the solar radiation change. The PMV model and Lai's model could reproduce the sudden variation in TSV; however, the changes in TSV were overestimated by the PMV model and underestimated by Lai's model.

Among the four evaluated models, Lai's model was the most accurate because its predictor variable *TL* (thermal load) considers heat gain due to solar radiation. Nevertheless, the

evaluation determined that none of the models was accurate, especially with sudden changes in solar radiation. A new model for predicting thermal sensation in cars should be developed to account for these sudden changes.

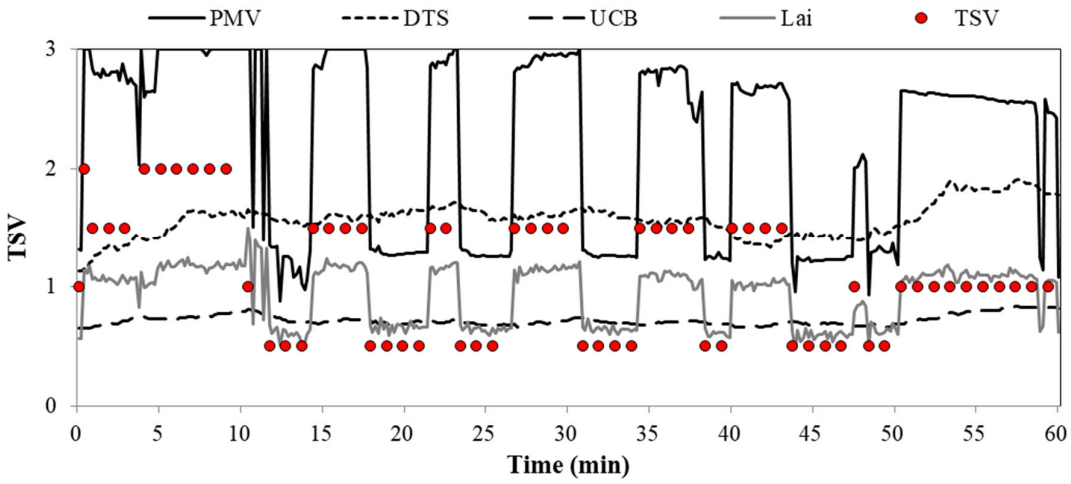

Fig. 8. Comparison between the actual thermal sensation and the predictions by the PMV, DTS and UCB models and Lai's model, with sudden changes in solar radiation.

3.3 Developing a thermal sensation model for a passenger car under driving conditions

Our new model is composed of two parts. After analyzing the relationship between thermal sensation and related parameters, the parameters that had the greatest association with thermal sensation were used to be the best predictor. The development of this part used data for parameters that do not reflect sudden changes in solar radiation. The second part of the model, meanwhile, considers the impact of sudden changes in solar radiation on thermal sensation, and was developed using thermal sensation votes.

3.3.1 Modeling the influence of gradually changing parameters

The first part of the model examines the influence of gradually changing parameters on thermal sensation. The first step of developing thermal sensation model was to select predictors. Gradual thermal load TL_g and skin temperature were reasonable candidates because TL_g indicates the general direction and magnitude of human heat transfer, and skin temperature is a good indicator of human thermal state due to the large number of thermoreceptors in the skin [45], [46], [47]. To find the best predictor, this study further examined the strengths of correlation between thermal sensation and thermal load and skin temperature at each segment and for the body as a whole. The parameters that had the greatest association with thermal sensation were then considered.

Table 7 presents the Pearson correlation coefficients between TSV and TL_g for different body segments. The TL_g for the face had the strongest correlation. Hagino et al. [52] observed that the overall thermal sensation is dominated by body parts that are directly exposed to

airflow and solar radiation. In addition, the face is an important organ for the whole body in dissipating heat. Hence, the face is highly sensitive to the thermal environment. Its gradual thermal load, TL_g *(face)*, was therefore selected as a predictor.

Table 7. Pearson correlation coefficients between thermal sensation and TL_g at different body segments and for the body as a whole. (n=1721)

TL_g	Face	Upper arm	Lower arm	Head	Whole body	Hand	Lower leg
Pearson correlation coefficient	0.74**	0.70**	0.67**	0.66**	0.58**	0.58**	0.57**

a. n=1721 (n=908 for summer, n=495 for winter and n=318 for shoulder season)
b. ** p<0.01.

Table 8 displays the Pearson correlation coefficients between TSV and skin temperature, including the mean skin temperature $T_{sk,m}$ and the skin temperature at different body segments. The mean skin temperature had the strongest correlation among all the skin temperatures because it integrated the thermoreceptor signals from all over the body. As a result, this investigation selected $T_{sk,m}$ as another predictor variable in the model.

Table 8. Pearson correlation coefficients between thermal sensation and local and mean skin temperatures. (n=1721)

Skin temperature	Mean skin	Lower arm	Face	Head	Upper arm	Upper leg	Lower leg
Pearson correlation coefficient	0.62**	0.57**	0.57**	0.53**	0.53**	0.48**	0.42**

a. n=1721 (n=908 for summer, n=495 for winter and n=318 for shoulder season)
b. ** p<0.01.

Thus, based on the above analysis, this study selected TL_g *(face)* and $T_{sk,m}$ to determine the thermal sensation when no sudden changes in solar radiation occur. Then, this study used the data set (n=732 for summer, n=394 for winter) to obtain the following relationship through multiple linear regressions:

Summer data (n=732):

$$TSV = 0.008 \cdot TL_g(face) + 0.333 \cdot T_{sk,m} - 11.370 \quad (R^2 = 0.78) \tag{16-1}$$

Winter data (n=394):

$$TSV = 0.01 \cdot TL_g(face) + 0.284 \cdot T_{sk,m} - 9.358 \quad (R^2 = 0.81) \tag{16-2}$$

Summer + winter data (n=1126):

$$TSV = 0.01 \cdot TL_g(face) + 0.216 \cdot T_{sk,m} - 7.352 \quad (R^2 = 0.78) \tag{16-3}$$

After analyzing the coefficients of multiple linear regression for the summer and winter data sets, it was found that the two data sets can be synthesized. A single model that can predict the thermal sensation in summer and winter conditions can be developed.

Using SPSS 24.0 [48] to analyze the experimental data, there was an approximately linear correlation (R^2 = 0.78) between the actual and predicted values by Eq. (16-3). Tables 9 and 10 show the hypothesis testing of the relation. There was no collinearity between the explanatory variables $T_{sk,m}$ and TL_g *(face)*.

Table 9. Anova for multiple linear regression equation (16-3).[a]

Model		Sum of squares	df	Mean square	F	Sig.
1	Regression	1659.272	2	829.636	2019.709	.000[b]
	Residual	461.295	1124	0.411		
	Total	2120.567	1126			

[a] Dependent Variable: TSV.
[b] Predictors: (Constant), $T_{sk,m}$, TL_g *(face)*.

Table 10. Coefficients for multiple linear regression equation (16-3).[a]

Model		Unstandardized coefficients		Standardized coefficients	t	Sig.	Collinear statistics	
		B	Std. error	Beta			Tolerance	VIF
1	(Constant)	-7.352	0.508		-14.483	0.000		
	TL_g (face)	0.01	0	0.707	39.873	0.000	0.615	1.625
	$T_{sk,m}$	0.216	0.015	0.25	14.092	0.000	0.615	1.625

[a] Dependent Variable: TSV.

3.3.2 Modeling the influence of sudden changes in solar radiation

Sudden changes in solar radiation resulted in changes in thermal sensation vote. Figure 9 summarizes the changes in thermal sensation vote (ΔTSV) corresponding to the changes in solar radiation thermal load (ΔTL_s) for the face, exposed surfaces other than the face, and non-exposed segments for all tested subjects in the shoulder season (n=318). The results exhibited reasonably good Pearson correlations of R = 0.96 ($p<0.01$), 0.81 ($p<0.01$), and 0.85 ($p<0.01$) for the face, other exposed surfaces, and surfaces of non-exposed segments, respectively. The high R for the face indicated that the ΔTL_s *(face)* could be used to evaluate ΔTSV.

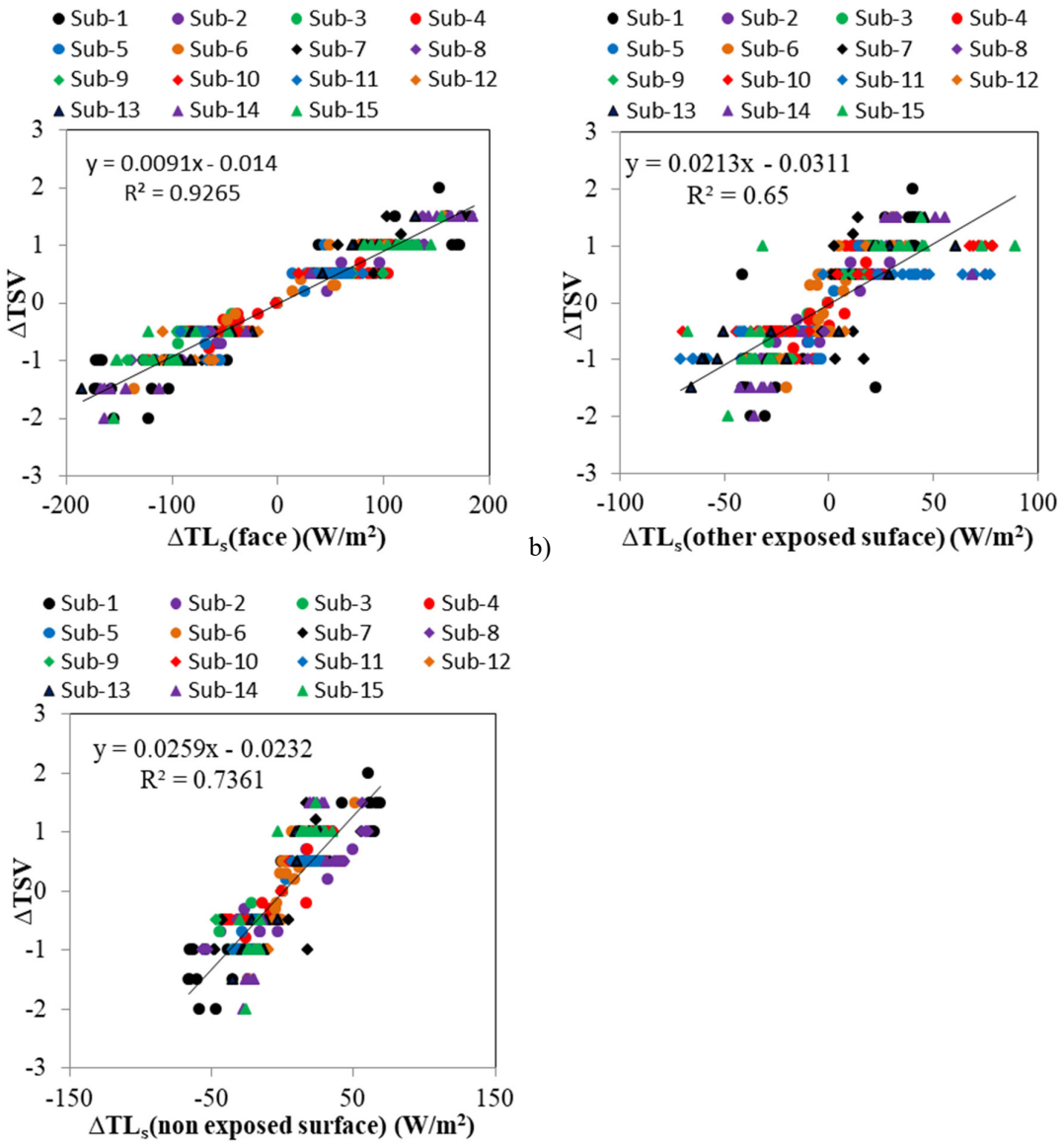

Fig. 9. Relationship between changes in solar radiation thermal load (ΔTL_s) and thermal sensation vote (ΔTSV) for all the subjects tested in the shoulder season for: (a) ΔTL_s (face); (b) ΔTL_s (other exposed surfaces); and (c) ΔTL_s (non-exposed surfaces).

Figure 10 shows similar relationships between *ΔTL_s (face)* and ΔTSV in summer, winter and the shoulder season. The green circles represent the relationship between ΔTSV and *ΔTL_s (face)* from summer. The change range of *ΔTL_s (face)* varied from (-176.9)-163.6 W/m^2 and the ΔTSV varied from (-2) to 2. The black diamonds represent data from winter. The change range of the *ΔTL_s (face)* varied from (-192.6)-178 W/m^2 and the ΔTSV varied from (-1) to 1. The red squares represent data from shoulder season. The change range of the *ΔTL_s (face)* varied from (-179)-181 W/m^2 and ΔTSV varied from (-1.5) to 1.5. The range of sudden changes in solar radiation was about the same, ranging from -180-180 W/m^2. But the changes of ΔTSV were different for different seasons.

Linear regression for ΔTSV for different seasons is:

$$\Delta TSV_{summer} = 0.0122 \cdot \Delta TL_s(face) + 0.0024 \quad (R^2=0.91) \quad (17\text{-}1)$$

$$\Delta TSV_{winter} = 0.0064 \cdot \Delta TL_s(face) \text{-} 0.0333 \quad (R^2=0.87) \quad (17\text{-}2)$$

$$\Delta TSV_{shoulder} = 0.0091 \cdot \Delta TL_s(face) \text{-} 0.014 \quad (R^2=0.93) \quad (17\text{-}3)$$

The slopes in linear regression equation (17-1, 17-2 and 17-3) differed between seasons. In summer, the driver's thermal perception was the most sensitive to changes in solar radiation, while the least sensitive in winter. This may due to differences in thermal expectation in different seasons. In the cold winter months, people desire solar radiation [50], [51] whereas in the summer, they tend to avoid strong sun [51].

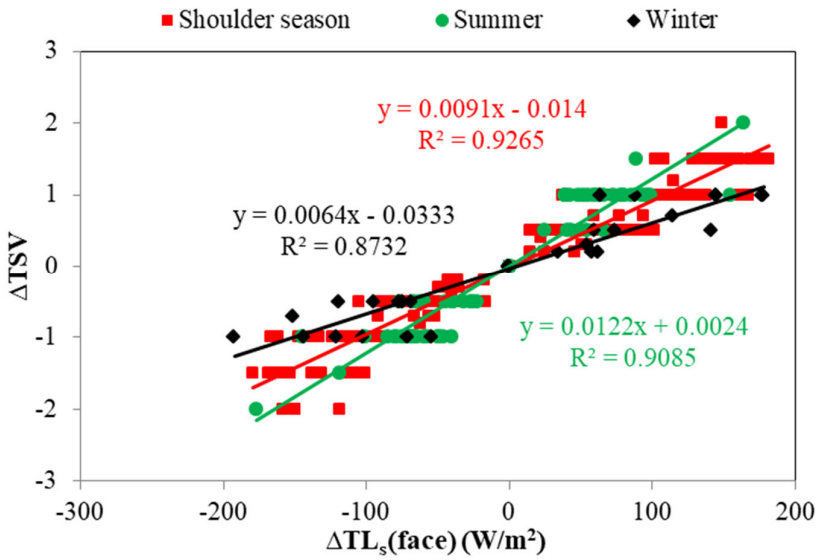

Fig. 10. Relationship between solar radiation thermal load (ΔTL_s) and thermal sensation votes (ΔTSV) in different seasons.

Next, Figure 11 reveals a strong correlation between the solar radiation thermal load needed to change TSV by one unit and the outdoor air temperature. The fitted linear equation provides the basis for estimating changes in TSV with respect to the outdoor air temperature:

$$\Delta TSV = \frac{\Delta TL_s(face)}{-3.0714 \cdot T_{out} + 166.8} \quad (18)$$

where T_{out} is the outdoor air temperature, ºC. Eq. (18) shows that an increase in outdoor air temperature leads to higher sensitivity on the part of TSV to changes in solar radiation. For example, when the T_{out} is 0 ºC in winter, a ΔTL_s *(face)* of 170 W/m^2 is required to bring a one-unit change in TSV. When the outdoor temperature is 30 ºC, a ΔTL_s *(face)* of only 80 W/m^2 is sufficient to change TSV by one unit.

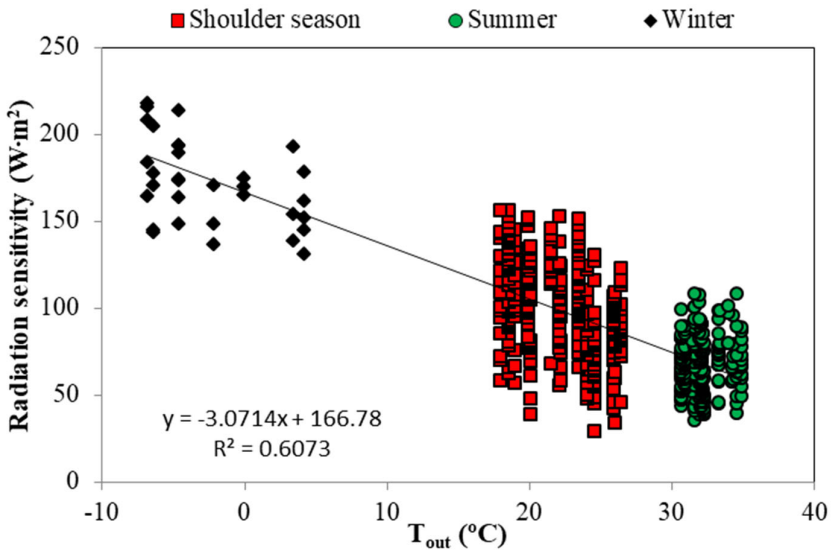

Fig. 11. Association between solar radiation thermal load needed to change TSV by one unit under different outdoor air temperatures, T_{out}.

When Eqs. (16-3) and (18) are combined, the thermal sensation model for cars under driving conditions becomes:

$$TSV = 0.01 \cdot TL_g(face) + 0.216 \cdot T_{sk,m} - 7.352 + \frac{\Delta TL_s(face)}{-3.0714 \cdot T_{out} + 166.8} \quad (19)$$

The first three terms on the right side of Eq. (19) represent the influence of gradually changing parameters, while the last term represents the influence of sudden changes in solar radiation. In addition, the influence of these sudden changes varies with outdoor air temperature.

Figure 12(a) compares the actual TSV and the TSV predicted by Eq. (16-3). The colored dots represent the votes under the influence of changing solar radiation during summer conditions and the colored squares during winter conditions. The predictions for TSV under changing solar radiation were not accurate. It can be seen that a large change in solar radiation gave rise to a large error. Meanwhile, Figure 12(b) compares the actual TSV with that predicted by Eq. (19). Almost all the colored dots and squares were within ±1 unit difference between the actual and predicted TSV.

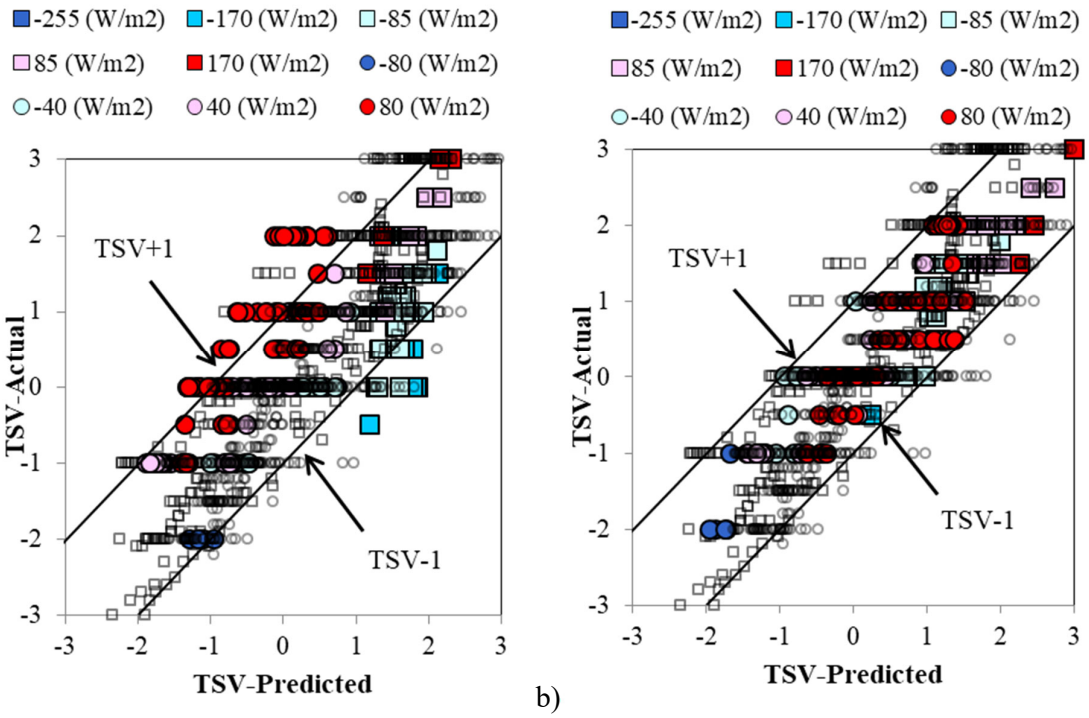

Fig. 12. Comparison between the actual TSV and the TSV predicted by: (a) Eq. (16-3) and (b) Eq. (19).

Table 11 shows the new model validation. The RMSE caused by the actual thermal sensation and the predicted value by equation (19) was 0.56, 0.66 and 0.30 for summer, winter and shoulder season, respectively. Compared to the new model, the four other models did not perform well for the summer and winter conditions, with a RMSE value larger than 1 thermal sensation unit (except Lai's model for winter data). When coming to the other two evaluation indices, the new model was 87.1% correct, Pearson R was 0.89 for all data (n=1721). Both of them showed more accurate than the other four models.

Table 11. Model validation results

	RMSE	Correct percentage (%)	Pearson R	p-value
Summer (n=908)	0.56	85.50	0.88	0.000
Winter (n=495)	0.66	82.00	0.89	0.000
Shoulder season (n=318)	0.30	100.00	0.86	0.000
All Data (n=1721)	0.56	87.10	0.89	0.000

4. Discussion

4.1 Effect of air velocity

For safety reasons, air velocity was only measured during the parking condition. Table 12 shows the measured air velocities. Due to the small space inside of the vehicle, the effect of

human presence cannot be ignored. The body blockage effects, induced self-convection, breathing airflow, and heat exchange with other bodies and even body parts can cause significant change in flow field patterns. There were 8 tests with two subjects seated in the front seats in summer. The passenger was an additional heat source that could also change the flow field. The change in airflow could lead to an error in TL_g *(face)*. The weather parameters also changed drastically that would also had an impact on airflow inside the vehicle. This investigation could not give quantitative estimate of the error.

Table 12. Local air velocities on different body segments (m/s).

	Face	Head	Thorax	Upper arm	Lower arm	Hand	Upper leg/Abdomen	Lower leg	Feet
Winter	0.17	0.16	0.11	0.12	0.07	0.31	0.11	0.52	0.52
Summer/ Shoulder season	0.46	0.33	0.73	0.31	0.26	1.56	0.22	0.10	0.10

4.2 *RS* and *RL* of different segments

As mentioned in section 2.1, the shortwave and longwave radiation was very complicated. Figure 13(a) shows that the shortwave radiant heat load obtained by different body segments varied greatly. *RS (face)* varied significantly from 5 to 173 W/m^2 during the exposure. *RS (lower leg)* varied only from 0 to 15 W/m^2. This was mainly because that the lower leg was blocked by surrounding structures and other body segments. Since the temperature of the interior wall of the vehicle does not change much (see Figure 6(b)), the longwave radiant heat load of each segment did not change much during the experiment (see Figure 13(b)). The change of the longwave radiant heat load on the face and head were the largest among all segments. The *RL (face)* and *RL (head)* varied with the surface temperature of center console and windshield due to the angle factor between face/head and surrounding surface center console/windshield. That was why we chose TL_g *(face)* and ΔTL_s *(face)* because they were most influential.

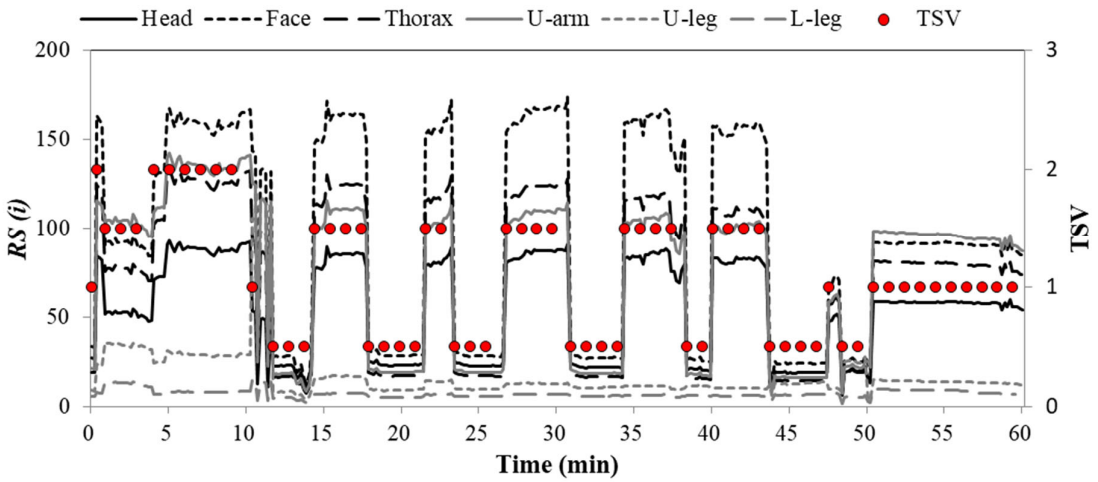

a)

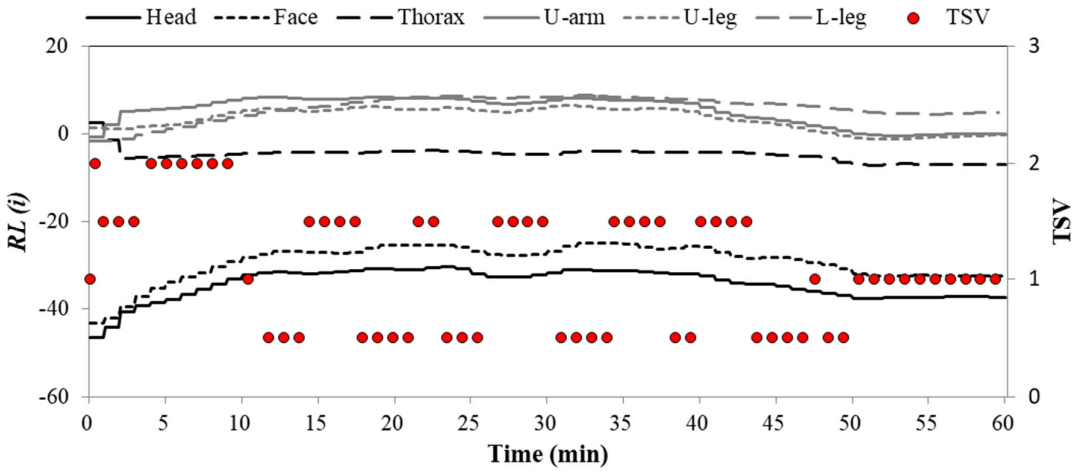

b)

Fig. 13. A tested case in the shoulder season: (a) Short-wave solar heat load, RS (i), (b) Long-wave heat load, RL (i) and thermal sensation vote, TSV.

4.3 Limitations and future challenges

The subject sample size was limited in this study, and the subjects did not encompass a wide variety of ages, weights, or other factors. Indraganti [49] found that thermal sensitivity changed with age, gender and economic group. Therefore, additional studies are needed to further validate the model developed here.

The core temperature of the human body is an important physiological parameter that influences thermal sensation. In practice, body core temperature is commonly monitored through rectal, esophageal, or tympanic measurements. Our experiment used the temperature measured by an ear thermometer to represent the core temperature of the body. However, perhaps because of the short duration of the experiment, the ear temperature changed only slightly during the tests. Therefore, we did not use the core temperature as a parameter for model development.

5. Conclusions

This investigation of thermal sensation conducted tests in cars under driving conditions with 32 participants in summer, 15 participants in winter, and 15 participants in the shoulder season. The study led to the following conclusions:

- The collected data was used to evaluate four commonly used thermal sensation models: the PMV model, the DTS model, the UCB model, and Lai's model. The evaluation results show none of the models was very accurate for driving conditions inside a car, because they did not consider the impact of changing solar radiation on thermal sensation.
- A sudden change in solar radiation in a car can greatly influence the thermal sensation of drivers. Drivers were more sensitive to changes in solar radiation under higher outdoor air temperature.

- This investigation developed a new model to predict thermal sensation in cars that uses gradual change in thermal load on the face, sudden change in solar radiation on the face, mean skin temperature and outdoor air temperature as predictors.
- The new model can predict thermal sensation in a car under driving conditions with an accuracy of 87.1% and with a RMSE less than 1 unit for all three outdoor driving conditions. The conditions were highly transient during the warm-up and cool-down phases in winter and summer, and sudden changes in solar radiation.

Acknowledgement

This study was supported by the National Key R&D Program of the Ministry of Science and Technology, China, on ″Green Buildings and Building Industrialization″ through Grant 2018YFC0705300.

References

[1] F. Norin, D.P. Wyon. Driver vigilance—The effects of compartment temperature. SAE Technical Papers 1992, International Congress and Exposition.

[2] A. Szczurek, M. Maciejewska. Categorisation for air quality assessment in car cabin. Transport & Environment 48 (2016) 161–170.

[3] P.O. Fanger. 1970. Thermal Comfort. Copenhagen: Danish Technical Press.

[4] ISO 7730 Ergonomics of the Thermal Environment – Analytical Determination and Interpretation of Thermal Comfort Using Calculation of the PMV and PPD Indices and Local Thermal Comfort Criteria.

[5] H. Zhang, E. Arens, C. Huizenga, T. Han. Thermal sensation and comfort models for non-uniform and transient environments: Part I: Local sensation of individual body parts. Building and Environment 45 (2010) 380–388.

[6] H. Zhang, E. Arens, C. Huizenga, T. Han. Thermal sensation and comfort models for non-uniform and transient environments, Part III: Whole-body sensation and comfort. Building and Environment 45 (2010) 399–410.

[7] H. Zhang. 2004. Human thermal sensation and comfort in transient and non-uniform thermal environments. Ph.D. Thesis. University of California at Berkeley, CA, USA.

[8] D. Fiala. 1998. Dynamic simulation of human heat transfer and thermal comfort. PhD thesis, De Montfort University, UK.

[9] D. Fiala, K. Lomas, M. Stohrer. First principles modeling of thermal sensation responses in steady-state and transient conditions. ASHRAE Transactions 109 (2003) 179–186.

[10] D. Fiala, G. Havenith, P. Bröde, et al. UTCI-Fiala multi-node model of human heat transfer and temperature regulation. Int J Biometeorol 56 (2012) 429–441.

[11] W. Zhang. 2013. Study on the key technology of thermal environment and occupant's thermal comfort in vehicles. Ph.D. Thesis. South China University of Tech, Guangdong, China.

[12] J.D. Ingersoll, T.G. Kalman, et al. Automobile passenger compartment thermal comfort model—Part II: Human thermal comfort calculation. SAE Paper Series (1992) 920266.

[13] K. Matsunaga, F. Sudo, S. Tanabe, T.L. Madsen. Evaluation and measurement of thermal comfort in the vehicles with a new thermal manikin. SAE Paper Series (1993) 931958.

[14] T. Han, K. Chen, B. Khalighi, et al. Assessment of various environmental thermal loads on passenger thermal comfort. SAE International Journal of Passenger Cars-Mechanical Systems 3 (2010) 2010-01-1205.

[15] A. Alahmer, M. Omar, A.R. Mayyas, A. Qattawi. Analysis of vehicular cabins' thermal sensation and comfort state, under relative humidity and temperature control, using Berkeley and Fanger models. Building and Environment 48 (2012) 146–163.
[16] M. Lorenz, D. Fiala, M. Spinnler, T. Sattelmayer. A Coupled numerical model to predict heat transfer and passenger thermal comfort in vehicle cabins. SAE Technical Paper (2014) 2014-01-0664.
[17] T. Han, K. Chen. Assessment of various environmental thermal loads on passenger compartment soak and cool-down analyses. SAE Technical Paper (2009) 2009-01-1148.
[18] J.H. Moon, W. Jin, H. Chan, et al. Thermal comfort analysis in a passenger compartment considering the solar radiation effect. International Journal of Thermal Sciences 107 (2016) 77–88.
[19] J.P. Rugh, R.B. Farrington, J.A. Boettcher. The Impact of Metal-free Solar Reflective Film on Vehicle Climate Control. SAE Technical Paper (2001). 2001-01-1721.
[20] J.P. Rugh, R.B. Farrington. Vehicle Ancillary Load Reduction Project Close-Out Report: An Overview of the Task and a Compilation of the Research Results, National Renewable Energy Laboratory. USA, Golden Publication, CO (2008).
[21] J. Rugh, L. Chaney, et al. (2013). Impact of Solar Control PVB Glass on Vehicle Interior Temperatures, Air-Conditioning Capacity, Fuel Consumption, and Vehicle Range. SAE 2013 World Congress & Exhibition. 2013-01-0553.
[22] S.G. Hodder, K. Parsons. The effects of solar radiation on thermal comfort. Int J Biometeorol 51 (2007) 233–250.
[23] Y. Ozeki, Y. Harita, A. Hirano, J. Nishihama. Evaluation on the solar reduction glass in an electric vehicle by experimental measurements in a climate chamber. SAE Technical Paper (2014) 2014-01-0703.
[24] ISO/TS 14505-1:2007. Ergonomics of the thermal environment—Evaluation of thermal environments in vehicles—Part 1: Principles and methods for assessment of thermal stress. Switzerland.
[25] ISO/TS 14505-2:2006. Ergonomics of the thermal environment—Evaluation of thermal environments in vehicles - Part 2: Determination of equivalent temperature. Switzerland.
[26] ISO/TS 14505-3:2006. Ergonomics of the thermal environment—Evaluation of thermal environments in vehicles - Part 3: Evaluation of thermal comfort using human subjects. Switzerland.
[27] C. Croitoru, I. Nastase, F. Bode, et al. Thermal comfort models for indoor spaces and vehicles-Current capabilities and future perspectives. Renewable & Sustainable Energy Reviews 44(2015) 304–318.
[28] P. Danca, A. Vartires, A. Dogeanu. An overview of current methods for thermal comfort assessment in vehicle cabin. Energy Procedia 85 (2016) 162–169.
[29] M. Paul, Rutkowski. Thermal comfort modeling of cooled automotive seats. SAE Technical Paper (2000) 2010-01-0552.
[30] X. Zhou, D. Lai, Q. Chen. Experimental investigation of thermal comfort in a passenger car under driving conditions. Building and Environment 149 (2019) 109–119.
[31] ASHRAE (2017) ASHRAE Handbook, Fundementals. American Society of Heating, Refrigerating and Air-conditioning Engineers, Inc., Atlanta.
[32] B.W. Olesen, Y. Hasebe, de Dear RJ (1988) Clothing insulation asymmetry and thermal comfort. ASHRAE Trans 94 (1) 32–51.
[33] F. Thellier, F. Monchoux, M. Bonnis-Sassi, B. Lartigue. Modeling additional solar constraints on a human being inside a room. Solar Energy 82 (2008) 290–301.
[34] Taitherm 12.6.0. Commercial Thermal Analysis Code. ThermoAnalytics Inc (2018).
[35] Y. Guan. 2002. Modeling of human thermal comfort for automobile applications under highly transient and non-uniform conditions. Ph.D. Thesis. University of Kansas State University, Kansas, USA.
[36] S. Tanabe, C. Narita, Y. Ozeki, M. Konishi. Effective radiation area of human body calculated by a numerical simulation. Energy and Buildings 32 (2000) 205–215.

[37] S. Tanabe, K. Kobayashi, J. Nakano, et al. Evaluation of thermal comfort using combined multi-node thermoregulation (65MN) and radiation models and computational fluid dynamics (CFD), Energy Build. 34 (2002) 637–646.
[38] G. Leduc, F. Monchoux, F. Thellier. Analysis of human's radiative exchange in a complex enclosure. Conference Paper. Moving Thermal Comfort Standards into the 21st Century, At Windsor, UK, 2001.
[39] D.A. McIntyre. Indoor Climate. Applied Science Publishers, London, Chap. 5.7: Scales of Warmth Sensation, p.134, 1980.
[40] D. Lai, Q. Chen. A two-dimensional model for calculating heat transfer in the human body in a transient and non-uniform thermal environment. Energy and Buildings 118 (2016) 114–122.
[41] D. Lai, X. Zhou, Q. Chen. Modelling dynamic thermal sensation of human subjects in outdoor environments. Energy and Buildings 149 (2017) 16–25.
[42] D. Lai, X. Zhou, Q. Chen. Measurements and predictions of the skin temperature of human subjects on outdoor environment. Energy and Buildings 151 (2017) 476–486.
[43] E. Foda, Kai Sirén. Dynamics of human skin temperatures in interaction with different indoor conditions. Conference Paper. June 2011.
[44] D. Wang, H. Zhang, et al. Observations of upper-extremity skin temperature and corresponding overall-body thermal sensations and comfort. Building and Environment 42 (2007) 3933–3943.
[45] Q. Jin, L. Duanmu, H. Zhang, et al.Thermal sensations of the whole body and head under local cooling and heating conditions during step-changes between workstation and ambient environment. Building and Environment 46 (2011) 2342–2350.
[46] P. Danca, A. Vartires, A. Dogeanu. An overview of current methods for thermal comfort assessment in vehicle cabin. Energy Procedia 85 (2016) 162–169.
[47] K. Imai, T. Kataoka, T. Masuda, T. Inada. New Evaluation method of transient and non-uniform environment in a passenger compartment. SAE 5 (2) (2012) 2012-01-0633.
[48] SPSS statistics 24, Rel. 24.0.0, SPSS Inc., Chicago (2016).
[49] M. Indraganti, K. Rao. Effect of age, gender, economic group and tenure on thermal comfort: A field study in residential buildings in hot and dry climate with seasonal variations. Energy and Buildings 42 (2010) 273–281.
[50] M. Xu, B. Hong, J. Mi, S. Yan. Outdoor thermal comfort in an urban park during winter in cold regions of China. Sustainable Cities and Society 43 (2018) 208–220.
[51] M. Nikolopouloua, S. Lykoudis. Use of outdoor spaces and microclimate in a Mediterranean urban area. Building and Environment 42 (2007) 3691–3707.
[52] M. Hagino, J. Hara. Development of a method for predicting comfortable airflow in the passenger compartment. SAE Technical Paper Series (1992) 922131.